Eur. Phys. J. C (2017) 77:103
DOI 10.1140/epjc/s10052-017-4657-4

THE EUROPEAN PHYSICAL JOURNAL C

Regular Article - Theoretical Physics

Radiative neutrino mass in alternative left–right model

Takaaki Nomura[1,a], **Hiroshi Okada**[2,b], **Yuta Orikasa**[1,3,c]

[1] School of Physics, KIAS, Seoul 130-722, Korea
[2] Physics Division, National Center for Theoretical Sciences, Hsinchu 300, Taiwan
[3] Department of Physics and Astronomy, Seoul National University, Seoul 151-742, Korea

Received: 9 September 2016 / Accepted: 16 January 2017 / Published online: 14 February 2017

Abstract We propose a radiative seesaw model in an alternative left–right model without any bidoublet scalar fields, in which all the fermion masses in the standard model are generated through a canonical seesaw mechanism at the tree level. On the other hand the observed neutrino masses are generated at two-loop level. In this paper we focus on the neutrino sector and show how to induce the active neutrino masses. Then we discuss the observed neutrino oscillation, constraints from lepton flavor violations, new sources of the muon anomalous magnetic moment, a long-lived dark matter candidate with keV scale mass, and collider physics.

1 Introduction

Current neutrino oscillation data provide strong evidence of tiny but nonzero neutrino masses [1]. Seesaw mechanism is one of the elegant realization to explain such tiny neutrino masses by introducing right-handed neutrinos, which can naturally be embedded into a left–right symmetry $SU(2)_{\rm L} \times SU(2)_{\rm R} \times U(1)_{B-L}$ as a theory at TeV scale [2].[1]

On the other hand, radiative seesaw models are also one of the natural realizations to explain the tiny neutrino masses at low energy scale where the neutrino mass matrix is generated at loop level, and a vast paper has recently been arisen in Refs. [3–120]. Moreover, some new particles such as dark matter (DM) and/or electrically charged particles, running inside a loop diagram, are introduced in radiative seesaw models. Thus the radiative seesaw models provide a wide variety of interesting phenomenologies correlated with neutrino sector, and these two scenarios are well compatible [14,15]. Thus it is an attractive interpretation that the active neutrino masses are generated by combination of these mechanisms since neutrino masses are very light compared to the other standard model (SM) fermions. In addition, implementing this scenario into left–right model will be phenomenologically interesting.

In this paper, we combine the left–right model and radiative seesaw model, in which active neutrino masses are generated at two-loop level while Dirac neutrino masses are generated at one loop, employing a specific left–right model based on Ref. [121].[2] A Majorana mass term of the right-handed neutrino is obtained at tree level by introducing $SU(2)_{\rm R}$ triplet scalar $\Delta_{\rm R}$. But we do not assume the exact left–right symmetry and $\Delta_{\rm L}$ is not introduced. Then we find allowed region of parameter spaces by carrying out numerical analysis where we take into account muon anomalous magnetic moment, various lepton flavor violating processes, and a long-lived DM candidate to explain the X-ray line at 7.1 keV [122,123], as well as consistency with the current neutrino oscillation data.

This paper is organized as follows. In Sect. 2, we show our model building including Higgs masses, neutrino mass matrix. In Sect. 3, we discuss lepton flavor violations (LFV), muon anomalous magnetic moment, DM, and collider physics and then carry out numerical analysis to search for the parameter space satisfying all the phenomenological constraints. We conclude in Sect. Appendix B.

2 The model

In this section, we introduce our model where the gauge symmetry is introduced as $SU(2)_{\rm L} \times SU(2)_{\rm R} \times U(1)_{\rm B-L}$. In this paper, we focus on the lepton sector and the details of the quark sector are found in Ref. [121].

[1] The left–right symmetry can smoothly be extended to larger groups, such as $SO(10)$ symmetry, which is typically realized at a higher scale such as in grand unified theories.

[2] The paper also discusses the quark sector.

[a] e-mail: nomura@kias.re.kr
[b] e-mail: macokada3hiroshi@cts.nthu.edu.tw
[c] e-mail: orikasa@kias.re.kr

Table 1 Lepton sector; notice the three flavor index of each field $L_{\mathrm{L(R)}}$ and $E_{\mathrm{L(R)}}$ is abbreviated

Fermion	L_{L}	L_{R}	$E_{\mathrm{L(R)}}$
$(SU(2)_{\mathrm{L}}, SU(2)_{\mathrm{R}}, U(1)_{\mathrm{B-L}})$	$(2, 1, -1)$	$(1, 2, -1)$	$(1, 1, -2)$

Table 2 Boson sector

Boson	Φ_{L}	Φ_{R}	h^+	Δ_{R}
$(SU(2)_{\mathrm{L}}, SU(2)_{\mathrm{R}}, U(1)_{\mathrm{B-L}})$	$(2, 1, 1)$	$(1, 2, 1)$	$(1, 1, 2)$	$(1, 3, 2)$

2.1 Particle contents and scalar sector

The particle contents for leptons and bosons are, respectively, shown in Tables 1 and 2. Here all the new fields are singlet under $SU(3)_{\mathrm{C}}$. We introduce $SU(2)_{\mathrm{R}}$ doublet fermions of L_{R} and isospin singlet vector-like fermions of $E_{\mathrm{L(R)}}$ both of which have three flavors like SM fermions. As for new bosons, we introduce two $SU(2)_{\mathrm{L(R)}}$ doublet scalars Φ_{L} and Φ_{R}, an isospin singlet singly charged scalar $h^{\pm}$, and an $SU(2)_{\mathrm{R}}$ triplet scalar Δ_{R}. Note here that Φ_{R} and Δ_{R}, respectively, develop vacuum expectation values (VEVs) (denoted by $v_{\mathrm{R}}/\sqrt{2}$ and $v_{\Delta}/\sqrt{2}$) in order to break the $SU(2)_{\mathrm{R}}$ symmetry and generate Majorana mass term for the right-handed neutrinos ν_{R} to realize seesaw mechanism with two-loop induced Dirac mass as shown below.

The relevant Lagrangian for Yukawa sector and scalar potential under these assignments are given by

$$\begin{aligned}-\mathcal{L}_{\mathrm{Y}} &= (h_{\mathrm{L}})_{ij}\bar{L}_{\mathrm{L}_i}\Phi_{\mathrm{L}}E_{\mathrm{R}_j} \\ &\quad + (h_{\mathrm{R}})_{ij}\bar{L}_{\mathrm{R}_i}\Phi_{\mathrm{R}}E_{\mathrm{L}_j} + (f_{\mathrm{L}})_{ij}\bar{L}^{C}_{\mathrm{L}_i}i\tau_2 L_{\mathrm{L}_j}h^{+} \\ &\quad + (f_{\mathrm{R}})_{ij}\bar{L}^{C}_{\mathrm{R}_i}i\tau_2 L_{\mathrm{R}_j}h^{+} \\ &\quad + (y_{\Delta_{\mathrm{R}}})_i\bar{L}^{c}_{\mathrm{R}_i}i\tau_2\Delta_{\mathrm{R}}L_{\mathrm{R}_i} + (M_{\mathrm{E}})_i\bar{E}_i E_i + \mathrm{c.c.}, \quad (2.1)\end{aligned}$$

$$\begin{aligned}\mathcal{V} &= -m^2_{\Phi_{\mathrm{L}}}|\Phi_{\mathrm{L}}|^2 - m^2_{\Phi_{\mathrm{R}}}|\Phi_{\mathrm{R}}|^2 - m^2_h|h^+|^2 - m^2_{\Delta}\mathrm{Tr}[|\Delta_{\mathrm{R}}|^2] \\ &\quad + \frac{\mu_2}{2}(\Phi^{\mathrm{T}}_{\mathrm{R}}i\tau_2\Delta^{\dagger}_{\mathrm{R}}\Phi_{\mathrm{R}} + \mathrm{h.c.}) \\ &\quad + \lambda_{\Phi_{\mathrm{L}}}|\Phi_{\mathrm{L}}|^4 + \lambda_{\Phi_{\mathrm{R}}}|\Phi_{\mathrm{R}}|^4 + \lambda_h|h^+|^4 + \lambda_{\Delta}(\mathrm{Tr}[|\Delta_{\mathrm{R}}|^2])^2 \\ &\quad + \lambda'_{\Delta}\mathrm{Tr}[|\Delta_{\mathrm{R}}|^4] + \lambda_{LR}|\Phi_{\mathrm{L}}|^2|\Phi_{\mathrm{R}}|^2 \\ &\quad + \lambda_{Lh}|\Phi_{\mathrm{L}}|^2|h^+|^2 + \lambda_{Rh}|\Phi_{\mathrm{R}}|^2|h^+|^2 \\ &\quad + \lambda_{h\Delta}|h^+|^2\mathrm{Tr}[|\Delta_{\mathrm{R}}|^2] + \lambda_{\Phi_{\mathrm{L}}\Delta}|\Phi_{\mathrm{L}}|^2\mathrm{Tr}[|\Delta_{\mathrm{R}}|^2] \\ &\quad + \lambda_{\Phi_{\mathrm{R}}\Delta}|\Phi_{\mathrm{R}}|^2\mathrm{Tr}[|\Delta_{\mathrm{R}}|^2] + \lambda'_{\Phi_{\mathrm{R}}\Delta}\Phi^{\dagger}_{\mathrm{R}}\Delta_R\Delta^{\dagger}_{\mathrm{R}}\Phi_{\mathrm{R}}, \quad (2.2)\end{aligned}$$

where τ_2 is a second component of the Pauli matrix, the index $i(j)$ runs 1–3, and $y_{\Delta_{\mathrm{R}}}$ and M_{E} can be diagonal without loss of the generality. It implies that $y_{\Delta_{\mathrm{R}}}$ does not contribute to lepton flavor violations. Notice here that each of $f_{\mathrm{L(R)}}$ and g should be antisymmetric and symmetric. We work on the basis where all the coefficients are real and positive for our brevity. After the left–right symmetry breaking, each of the scalar fields has nonzero mass. We parametrize these scalar fields by

$$\Phi_{\mathrm{L(R)}} = \begin{bmatrix}\phi^{+}_{\mathrm{L(R)}} \\ \phi^{0}_{\mathrm{L(R)}}\end{bmatrix}, \quad \phi^{0}_{\mathrm{L(R)}} = \frac{1}{\sqrt{2}}(v_{\mathrm{L(R)}} + h_{\mathrm{L(R)}} + ia_{\mathrm{L(R)}}), \quad (2.3)$$

$$\Delta_{\mathrm{R}} = \begin{bmatrix}\frac{\Delta^{+}}{\sqrt{2}} & \Delta^{++} \\ \Delta^{0} & -\frac{\Delta^{+}}{\sqrt{2}}\end{bmatrix}, \quad \Delta^{0} = \frac{1}{\sqrt{2}}(v_{\Delta} + \Delta^{0}_{\mathrm{R}} + i\Delta^{0}_{I}), \quad (2.4)$$

where h_{L} is the SM-like Higgs, and v_{L} is related to the Fermi constant G_{F} by $v^2_{\mathrm{L}} = 1/(\sqrt{2}G_{\mathrm{F}}) \approx (246\ \mathrm{GeV})^2$. The VEVs of $\Phi_{\mathrm{L(R)}}$ are derived from the conditions $\partial\mathcal{V}/\partial v_{\mathrm{L}} = 0$, $\partial\mathcal{V}/\partial v_{\mathrm{R}} = 0$ and $\partial V/\partial v_{\Delta} = 0$ such that

$$\begin{aligned}v^2_{\mathrm{L}} &\simeq \frac{1}{\lambda_{\Phi_{\mathrm{L}}}}\left(m^2_{\Phi_{\mathrm{L}}} - \frac{\lambda_{\mathrm{LR}}}{2}v^2_{\mathrm{R}}\right), \\ v^2_{\mathrm{R}} &\simeq \frac{1}{\lambda_{\Phi_{\mathrm{R}}}}\left(m^2_{\Phi_{\mathrm{R}}} - \frac{\lambda_{\mathrm{LR}}}{2}v^2_{\mathrm{L}}\right), \quad (2.5)\end{aligned}$$

$$v^2_{\Delta} \simeq -\frac{1}{2\sqrt{2}}\frac{\mu_2 v^2_{\mathrm{R}}}{m^2_{\Delta}}. \quad (2.6)$$

In this paper we require $v_{\mathrm{R}} \gg v_{\mathrm{L}}$, which can be obtained if we adopt $m^2_{\Phi_{\mathrm{R}}}/\lambda_{\Phi_{\mathrm{R}}} \gg m^2_{\Phi_{\mathrm{L}}}/\lambda_{\Phi_{\mathrm{L}}}$ and choose rather small value of λ_{LR}. After the symmetry breaking, we have massive gauge bosons $W^{\pm}_{\mathrm{L(R)}}$ and $Z_{\mathrm{L(R)}}$ associated with left–right symmetry. Note that a neutral singlet scalar is required to obtain the desired symmetry breaking pattern in the model of Ref. [121], while we can realize the symmetry breaking due to the absence of exact left–right symmetry in the scalar potential.

The CP even Higgs boson mass matrix in the basis of $(h_{\mathrm{L}}, h_{\mathrm{R}}, \Delta^0_{\mathrm{R}})$ is denoted by $(M^2)_{\text{CP-even}}$, and it is diagonalized by 3×3 orthogonal mixing matrix O_{R} as $O_{\mathrm{R}}(M^2)_{\text{CP-even}}O^{\mathrm{T}}_{\mathrm{R}} = \mathrm{diag.}(m^2_{h_1}, m^2_{h_2}, m^2_{h_3})$. Thus $h_{\mathrm{L(R)}}$ and Δ^0_{R} are, respectively, given by

$$\begin{aligned}h_{\mathrm{L}} &\equiv \sum_{a=1-3}(O^{\mathrm{T}}_{\mathrm{R}})_{1a}h_a, \quad h_{\mathrm{R}} \equiv \sum_{a=1-3}(O^{\mathrm{T}}_{\mathrm{R}})_{2a}h_a, \\ \Delta^0_{\mathrm{R}} &\equiv \sum_{a=1-3}(O^{\mathrm{T}}_{\mathrm{R}})_{3a}h_a, \quad (2.7)\end{aligned}$$

where $h_1 \equiv h_{\rm SM}$ is the SM Higgs and $h_{2,3}$ are additional CP even Higgs mass eigenstates.

The CP odd component $a_{\rm L}$ from $\Phi_{\rm L}$ does not mix with the other CP odd components. Thus $a_{\rm L}$ is the massless Nambu–Goldstone (NG) boson which is absorbed by $Z_{\rm L}$ boson. The CP odd Higgs boson mass matrix in the basis of $(\Delta_I^0, a_{\rm R}^0)$ is denoted by $(M^2)_{\text{CP-odd}}$, and it is diagonalized by 2×2 orthogonal mixing matrix O_I as $O_I (M^2)_{\text{CP-odd}} O_I^{\rm T} = \text{diag.}(m_{A_1}^2, m_{A_2}^2)$. Therefore $a_{\rm R}$ and Δ_I are given by

$$a_{\rm R} \equiv \sum_{a=1-2} (O_I^{\rm T})_{1a} A_a, \quad \Delta_I \equiv \sum_{a=1-2} (O_I^{\rm T})_{2a} A_a, \tag{2.8}$$

where only A_1 should be massive, since A_2 is absorbed by the $Z_{\rm R}$ boson.

The singly charged scalar boson h^+ does not mix with other charged scalar bosons. Thus it is the mass eigenstate with mass $m_{h^\pm}$. Also the singly charged component $\phi_{\rm L}^\pm$ from $\Phi_{\rm L}$ does not mix and it is the massless NG boson absorbed by $W_{\rm L}^\pm$. The singly charged scalar boson mass matrix in the basis of $(\Delta^\pm, \phi_{\rm R}^\pm)$ is denoted by $(M^2)_{\rm singly}$, and it is diagonalized by the 2×2 unitary mixing matrix U_1 as $U_1 (M^2)_{\rm singly} U_1^\dagger = \text{diag.}\ (m_{\phi_1^\pm}^2, m_{\phi_2^\pm}^2)$. Therefore $\Delta^\pm$ and $\phi_{\rm R}^\pm$ are given by

$$\Delta^\pm \equiv \sum_{a=1-2} (U_1^\dagger)_{1a} \phi_a^\pm, \qquad \phi_{\rm R}^\pm \equiv \sum_{a=1-2} (U_1^\dagger)_{2a} \phi_a^\pm, \tag{2.9}$$

where $m_{\phi_2^\pm}^2$ should be zero, since $\phi_2^\pm$ is absorbed by $W_{\rm R}^\pm$ boson. The doubly charged scalar boson $\Delta^{\pm\pm}$ is mass eigenstate with mass eigenvalue $m_{\Delta^{\pm\pm}} \simeq m_\Delta$.

2.2 Charged lepton sector

First of all, we define the isospin doublet fermions as $L_{\rm L(R)} \equiv [\nu_{\rm L(R)}, \ell_{\rm L(R)}]^{\rm T}$. The charged lepton mass matrix in the basis of (ℓ, E) can be given as

$$M_\ell = \begin{bmatrix} 0 & h_{\rm L} v_{\rm L}/\sqrt{2} \\ h_{\rm R}^{\rm T} v_{\rm R}/\sqrt{2} & M_{\rm E} \end{bmatrix} \equiv \begin{bmatrix} 0 & m_{\rm L} \\ m_{\rm R}^{\rm T} & M_{\rm E} \end{bmatrix}. \tag{2.10}$$

Then it can be diagonalized by bi-unitary mixing matrix $V_{\rm L}$ and $V_{\rm R}$ as $V_{\rm L} M_\ell V_{\rm R}^{\rm T} = M_{\rm diag}$, where

$$V_{\rm L} M_\ell V_{\rm R}^{\rm T} \approx \begin{bmatrix} -m_{\rm L} M_{\rm E}^{-1} m_{\rm R} & 0 \\ 0 & M_{\rm E} \end{bmatrix}, \tag{2.11}$$

$$V_a \approx \begin{bmatrix} 1 - \frac{\rho_a \rho_a^{\rm T}}{2} & -\rho_a \\ \rho_a^{\rm T} & 1 - \frac{\rho_a^{\rm T} \rho_a}{2} \end{bmatrix}, \quad \rho_{\rm L} = m_{\rm L} M_{\rm E}^{-1},$$
$$\rho_{\rm R} = m_{\rm R}^{\rm T} M_{\rm E}^{-1}, \quad a = L, R. \tag{2.12}$$

Here we have used the assumption $m_{\rm L}, m_{\rm R} << M_{\rm E}$. The resultant charged lepton mass squared is then given by

$$|m_\ell|_{ij}^2 \approx m_{\rm L} M_{\rm E}^{-1} m_{\rm R} m_{\rm R}^\dagger (M_{\rm E}^{-1}) m_{\rm L}^\dagger$$
$$= \frac{v_{\rm L}^2 v_{\rm R}^2}{4} h_{\rm L} M_{\rm E}^{-1} h_{\rm R} h_{\rm R}^\dagger M_{\rm E}^{-1} h_{\rm L}^\dagger$$
$$\approx \frac{v_{\rm L}^2}{4} |h_{\rm L} h_{\rm R}|^2, \tag{2.13}$$

if we assume to be $M_{\rm E} \approx v_{\rm R}$.

2.3 Neutrino sector

The neutral fermion mass matrix in the basis of $(\nu_{\rm L}, \nu_{\rm R})$ is generated by

$$(\mathcal{M}_\nu)_{ab} = \begin{bmatrix} 0 & m_{\rm D} \\ m_{\rm D}^{\rm T} & m_{\nu_{\rm R}} \end{bmatrix}, \tag{2.14}$$

where $m_{\nu_{\rm R}} \equiv y_{\Delta_{\rm R}} v_\Delta / \sqrt{2} = \text{diag.}(m_{N_1}, m_{N_2}, m_{N_3})$,[3] and the Dirac fermion mass matrix $m_{\rm D}$ is given by

$$m_{\rm D} \approx \frac{v_{\rm L} v_{\rm R} (F_{\rm L})_{i\alpha}^1 (h_{\rm L})_{\alpha a} (h_{\rm R}^{\rm T})_{a\beta} (F_{\rm R}^{\rm T})_{\beta j}^1}{2\pi^2 M_{E_a}} \frac{\ln Z_{a,1}}{1 - Z_{a,1}}, \tag{2.15}$$

where all the indices are summed over, and we define $(F_{L/R})_{ij}^a \equiv (U_1^\dagger)_{1a} (f_{L/R})_{ij}$, $Z_{a,\rho} \equiv \left(\frac{m_{h_\rho^\pm}}{M_{E_a}} \right)^2$, and assume to be $m_\ell << M_{\rm E}$. Therefore the active neutrino masses can be obtained at two-loop level through two types of the seesaw mechanisms (canonical seesaw with one-loop induced Dirac mass and its irreducible diagram [34]); $(\mathcal{M}_\nu)_{ab} \approx m_{\rm D} m_{\nu_{\rm R}}^{-1} m_{\rm D}^{\rm T}$.[4] Notice here that one of three neutrino masses is zero without loss of the generality, because the matrix rank of $(m_{\rm D})_{3\times 3}$ is two.

Then $(\mathcal{M}_\nu)_{ab}$ is diagonalized by the Maki–Nakagawa–Sakata mixing matrix $V_{\rm MNS}$ (MNS) as

$$(\mathcal{M}_\nu)_{ab} = (V_{\rm MNS} D_\nu V_{\rm MNS}^{\rm T})_{ab}, \quad D_\nu \equiv (m_{\nu_1}, m_{\nu_2}, m_{\nu_3}), \tag{2.16}$$

$$V_{\rm MNS} = \begin{bmatrix} c_{13} c_{12} & c_{13} s_{12} & s_{13} e^{-i\delta} \\ -c_{23} s_{12} - s_{23} s_{13} c_{12} e^{i\delta} & c_{23} c_{12} - s_{23} s_{13} s_{12} e^{i\delta} & s_{23} c_{13} \\ s_{23} s_{12} - c_{23} s_{13} c_{12} e^{i\delta} & -s_{23} c_{12} - c_{23} s_{13} s_{12} e^{i\delta} & c_{23} c_{13} \end{bmatrix}, \tag{2.17}$$

where we neglect the Dirac phase δ as well as the Majorana phase in the numerical analysis for simplicity. We present

[3] Our main motivation to introduce the $SU(2)_{\rm R}$ triplet boson $\Delta_{\rm R}$ is to formulate the seesaw neutrino mass matrix appropriately. Actually even if $\Delta_{\rm R}$ is not introduced, a rather heavier right-handed neutrino mass matrix $m_{\nu_{\rm R}}$ can be induced at the two-loop level by increasing the scale of $v_{\rm R}$. However, we cannot define the inverse of the seesaw neutrino mass matrix, because the matrix rank is reduced by one. Therefore, the seesaw formula does not work well.

[4] The loop function with the irreducible diagram is usually smaller than the one with the canonical seesaw diagram [68]. Thus we consider the canonical seesaw type model only.

the following neutrino oscillation data at 95% confidence level [124]:

$$\begin{aligned} &0.2911 \le s^2_{12} \le 0.3161,\ 0.5262 \le s^2_{23} \le 0.5485,\\ &0.0223 \le s^2_{13} \le 0.0246,\\ &|m^2_{\nu_3} - m^2_{\nu_2}| = (2.44 \pm 0.06) \times 10^{-3}\ \mathrm{eV}^2,\\ &m^2_{\nu_2} - m^2_{\nu_1} = (7.53 \pm 0.18) \times 10^{-5}\ \mathrm{eV}^2, \end{aligned} \tag{2.18}$$

where we assume normal ordering of the neutrino mass eigenstate in our analysis below; therefore $m_{\nu_1} = 0$.

2.4 Neutrinoless double beta decay

Here we discuss the non-standard contribution to the neutrinoless double beta decay. The relevant process arises from the same process of the standard interaction just by flipping the chirality $L \to R$, and its formula is given by

$$\begin{aligned} m_{\beta\beta} &= \left| \sum_{i=1}^{3} |(V^2_{\mathrm{MNS}})_{1i}| m_{\nu_i} + \left[\frac{m_{W_\mathrm{L}}}{m_{W_\mathrm{R}}}\right]^4 \left[\frac{g_\mathrm{L}}{g_\mathrm{R}}\right]^4 m_{\nu_{R_1}} \right| \\ &= \left| \sum_{i=1}^{3} |(V^2_{\mathrm{MNS}})_{1i}| m_{\nu_i} + \frac{v^4_\mathrm{L}}{(v^2_\mathrm{R} + 2v^2_\Delta)} m_{\nu_{R_1}} \right|, \end{aligned} \tag{2.19}$$

where the first term in the left side equation is the contribution to the SM and the second term is the one of the new contribution. Furthermore we have used $m_{W_\mathrm{L}} = g_\mathrm{L} v_\mathrm{L}/2$, $m_{W_\mathrm{R}} = g_\mathrm{R}\sqrt{v^2_\mathrm{R} + 2v^2_\Delta}/2$, and the mixing among ν_Rs is assumed to be diagonal for simplicity. When we adopt the typical bound $m_{\beta\beta} \lesssim 0.29$ eV [125], we can estimate the upper bound on the mass of ν_{R_1} once the v_R and v_Δ are fixed. We will see a concrete discussion in the section of numerical analysis.

3 Phenomenology of the model

In this section, we discuss some phenomenologies in our model such as LFV, muon anomalous magnetic moment and DM. Then numerical analysis is carried out to search for allowed parameter space which is consistent with current experimental data.

3.1 Muon anomalous magnetic moment and Lepton flavor violations

The muon anomalous magnetic moment (muon $g-2$) has been measured at Brookhaven National Laboratory. The current average of muon $g-2$ experimental results is found as [126]

$$a^{\mathrm{exp}}_\mu = 11659208.0(6.3) \times 10^{-10}.$$

Two discrepancy between the experimental data and the prediction in SM; $\Delta a_\mu \equiv a^{\mathrm{exp}}_\mu - a^{\mathrm{SM}}_\mu$, have, respectively, been computed in Ref. [127] as

$$\Delta a_\mu = (29.0 \pm 9.0) \times 10^{-10} \text{ at } 3.2\sigma \text{ C.L.}, \tag{3.1}$$

and in Ref. [128] as

$$\Delta a_\mu = (33.5 \pm 8.2) \times 10^{-10} \text{ at } 4.1\sigma \text{ C.L.} \tag{3.2}$$

In our model, we have new contributions to Δa_μ coming from the Yukawa coupling of $h_{\mathrm{L(R)}}$ and $f_{\mathrm{L(R)}}$, and its contribution is given as[5]

$$\Delta a_\mu \approx \Delta a^{h_H}_\mu + \Delta a^{h_A}_\mu + \Delta a^{f}_\mu + \Delta a^{\Delta}_\mu, \tag{3.3}$$

$$\Delta a^{h_H}_\mu \approx \frac{m_\mu}{2(4\pi)^2} \sum_{\alpha=1}^{3}\sum_{a=1}^{3} \left[\frac{(H^a)_{2\alpha}(H^\dagger_a)_{\alpha 2}}{M_{E_\alpha}} \times \frac{1 + 3Y^2_{\alpha,a} - 4Y_{\alpha,a} - 2Y^2_{\alpha,a}\ln[Y_{\alpha,a}]}{(1 - Y_{\alpha,a})^3} \right], \tag{3.4}$$

$$\Delta a^{h_A}_\mu \approx -\frac{1}{(4\pi)^2} (m_\mu)^2 \sum_{\alpha=1}^{3}\sum_{a=1}^{3} \frac{(H'^a)^*_{\alpha,2}(H'^a)_{\alpha,2}}{M^2_{E_\alpha}} F_2\left(Y'_{\alpha,a}\right), \tag{3.5}$$

$$\Delta a^{f}_\mu \approx -\frac{m^2_\mu}{3(4\pi)^2 m^2_{h^\pm}} \times \sum_{\alpha,\beta=1}^{3} \left[(f^\dagger_\mathrm{L})_{2\alpha}(f_\mathrm{L})_{\alpha 2} + (f^\dagger_\mathrm{R})_{2\beta}(f_\mathrm{R})_{\beta,2} F_2(\epsilon_\beta) \right], \tag{3.6}$$

$$\Delta a^{\Delta}_\mu \approx -\frac{m^2_\mu}{4(4\pi)^2} \sum_{\alpha,\beta=1}^{3} \left[\frac{(y^\dagger_{\Delta_\mathrm{R}})_{2\alpha}(y_{\Delta_\mathrm{R}})_{\alpha 2}}{m^2_{\Delta^{\pm\pm}}} + \sum_{b=1}^{2} \frac{(Y^{b\dagger}_{\Delta_1})_{2\beta}(Y^b_{\Delta_1})_{\beta 2}}{6m^2_{h^\pm_b}} F_2(\epsilon^b_\beta) \right], \tag{3.7}$$

$$F_2(x) \equiv \frac{1 - 6x + 3x^2 + 2x^3 - 6x^2\ln x}{(1-x)^4}, \tag{3.8}$$

where we define $H^a_{ij} \equiv \frac{(h_\mathrm{L})_{ij}(O^\mathrm{T}_\mathrm{R})_{1a} + (h_\mathrm{R})_{ij}(O^\mathrm{T}_\mathrm{R})_{2a}}{2\sqrt{2}}$, $H'^a_{ij} \equiv \frac{(O^\mathrm{T}_I)_{1a}(h_\mathrm{R})_{ij}}{\sqrt{2}}$, $Y_{\alpha,a} \equiv (m_{h^0_a}/M_{E_\alpha})^2$, $Y'_{\alpha,a} \equiv m^2_{A_a}/M^2_{E_\alpha}$, $\left(Y_{\Delta_1}\right)_{a\alpha} \equiv (U^\dagger_1)_{2a}(y_{\Delta_\mathrm{R}})_\alpha$, $\epsilon^{(b)}_j \equiv (m_{\nu_{\mathrm{R}_j}}/m_{h^\pm_{(b)}})^2$ and we have assumed $m_{\nu_\mathrm{L}} << m_\ell << \{m_{\nu_\mathrm{R}}, M_\mathrm{E}, m_{h^0_a}, m_{h^\pm_{(b)}}\}$. Note here that the contribution of Δa^Δ_μ is negligibly small because of the small mixing.

Lepton flavor violation processes (*LFVs*) $\ell_i \to \ell_j\gamma$ and $\ell^-_i \to \ell^-_j\ell^+_k\ell^-_\ell$ at the one-loop level are measured precisely

[5] Useful formulas for the muon $g-2$ can be found in Ref. [129].

Table 3 Summary of $\ell_i \to \ell_j \gamma$ process and the lower bound of experimental data [130]

Process	(i, j)	Experimental bounds (90% CL)
$\mu^- \to e^-\gamma$	(2, 1)	$\mathrm{Br}(\mu \to e\gamma) < 5.7 \times 10^{-13}$
$\tau^- \to e^-\gamma$	(3, 1)	$\mathrm{Br}(\tau \to e\gamma) < 3.3 \times 10^{-8}$
$\tau^- \to \mu^-\gamma$	(3, 2)	$\mathrm{Br}(\tau \to \mu\gamma) < 4.4 \times 10^{-8}$

and severely constrained. Each of flavor dependent process has to satisfy the current upper bound, as can be seen in Tables 3 and 4. The branching ratio (BR) for the $\ell_i \to \ell_j \gamma$ can be written as

$$\begin{aligned}
&\mathrm{Br}(\ell_i \to \ell_j \gamma) = \frac{48\pi^3 \alpha_{\mathrm{em}} C_i}{m_{\ell_i}^2 {\mathrm{G_F}}^2}(|a_{\mathrm{L}}|^2 + |a_{\mathrm{R}}|^2),\\
&a_{\mathrm{L}} = a_h + a_{f_{\mathrm{R}}}, \quad a_{\mathrm{R}} = a_h + a_{f_{\mathrm{L}}}, \qquad (3.9)\\
&a_h \approx -\frac{1}{2(4\pi)^2}\sum_{\alpha=1}^{3}\sum_{a=1}^{3}\frac{(H^a)_{i\alpha}(H_a^\dagger)_{\alpha j}}{M_{E_\alpha}}\\
&\qquad \times \frac{1 + 3Y_{\alpha,a}^2 - 4Y_{\alpha,a} - 2Y_{\alpha,a}^2 \ln[Y_{\alpha,a}]}{(1 - Y_{\alpha,a})^3}, \qquad (3.10)\\
&a_{f_{\mathrm{R}}} \approx m_{\ell_i}\sum_{\alpha=1}^{3}\frac{(f_{\mathrm{R}}^\dagger)_{j\alpha}(f_{\mathrm{R}})_{\alpha i}}{3(4\pi)^2 m_{h^\pm}^2} F_2(\epsilon_\alpha),\\
&a_{f_{\mathrm{L}}} \approx m_{\ell_i}\sum_{\alpha=1}^{3}\frac{(f_{\mathrm{L}}^\dagger)_{j\alpha}(f_{\mathrm{L}})_{\alpha i}}{3(4\pi)^2 m_{h^\pm}^2}, \qquad (3.11)
\end{aligned}$$

where $C_i \approx (1, 1/5)$ for $i = (\mu, \tau)$ [131], $\mathrm{G_F}$ is Fermi constant, and α_{em} is the fine-structure constant. On the other hand, the BR for the process $\ell_i^- \to \ell_j^- \ell_k^+ \ell_\ell^-$ is given by

$$\begin{aligned}
&\mathrm{Br}(\ell_i^- \to \ell_j^- \ell_k^+ \ell_\ell^-)\\
&\approx \frac{C_i}{16{\mathrm{G_F}}^2}\Big(8|A|^2 + 8|B|^2 + 2|C|^2 + 2|D|^2\\
&\quad +2|A_{\mathrm{L}}|^2 + 2|B_{\mathrm{L}}|^2 + 2|A_{\mathrm{R}}|^2 + 2|B_{\mathrm{R}}|^2 + |C_{\mathrm{R}}|^2\\
&\quad -8\mathrm{Re}[AB^*] + 4\mathrm{Re}[AD^*] + 4\mathrm{Re}[BC^*] + \mathrm{Re}[CD^*]\\
&\quad -4\mathrm{Re}[AA_{\mathrm{L}}^*] + 4\mathrm{Re}[AB_{\mathrm{L}}^*] - 4\mathrm{Re}[AA_{\mathrm{R}}^*]\\
&\quad +4\mathrm{Re}[AB_{\mathrm{R}}^*] + 4\mathrm{Re}[AC_{\mathrm{R}}^*] + 4\mathrm{Re}[BA_{\mathrm{L}}^*] - 4\mathrm{Re}[BB_{\mathrm{L}}^*]\\
&\quad +4\mathrm{Re}[BA_{\mathrm{R}}^*] - 4\mathrm{Re}[BB_{\mathrm{R}}^*] - 4\mathrm{Re}[BC_{\mathrm{R}}^*] - 4\mathrm{Re}[A_{\mathrm{L}}B_{\mathrm{L}}^*]\\
&\quad -4\mathrm{Re}[A_{\mathrm{R}}B_{\mathrm{R}}^*] - 4\mathrm{Re}[A_{\mathrm{R}}C_{\mathrm{R}}^*] + 4\mathrm{Re}[B_{\mathrm{R}}C_{\mathrm{R}}^*]\\
&\quad +8\mathrm{Re}[BE^*] + 8\mathrm{Re}[BF^*] + \mathrm{Re}[CE^*]\\
&\quad +\mathrm{Re}[CF^*] + \frac{1}{2}|E|^2 + \frac{1}{2}|F|^2\Big), \qquad (3.12)
\end{aligned}$$

where the numerical factors $\{A, B, C, D\}$ come from box loop diagrams in which E_α and h_a are running while the other factors come from box loop diagrams with E_α, h_a and A_a running inside the loop; the explicit forms of these factors are given in Appendix B. Note that the LFV decay ratios are determined by the Yukawa couplings $h_{\mathrm{L(R)}}$ and $f_{\mathrm{L(R)}}$ which also appear in our neutrino mass formula Eq. (2.15) indicating the correlation between LFV and neutrino mass matrix.

3.2 Dark matter

We consider a fermionic DM candidate $X(\equiv \nu_{\mathrm{R}_1})$, which is assumed to be the lightest particle of ν_{R_i}. Since DM can decay into neutrinos and photon through the Dirac mass term at the one-loop level, DM has to be long-lived. Hence we focus on the explanation of the X-ray line at 3.55 keV, since X decays into active neutrinos and photon at the one-loop level after the symmetry breaking. Then the mass of DM $M_X(\equiv M_{\nu_{\mathrm{R}_1}})$ is fixed to be around 7.1 keV with a small value of the decay rate divided by M_X; *i.e.*, $4.8 \times 10^{-48} \lesssim \frac{\Gamma(X \to \nu_k \gamma)}{M_X} \lesssim 4.6 \times 10^{-46}$ [134].[6] We also note that such a DM candidate will be over-abundant if one estimates thermal relic density through the gauge interactions. However, this problem can be evaded by the entropy production due to the late decay of $\nu_{R_{2,3}}$ [132,133]. In our analysis, we assume the right relic density can be obtained by this mechanism and the constraints on the decay rate of DM is taken into account. Then the decay rate is derived as

$$\begin{aligned}
&\frac{\Gamma(X \to \nu_k \gamma)}{M_X}\\
&\approx \frac{\alpha_{\mathrm{em}} a b_j}{16\pi^4}\left|\sum_{j}^{1-3}(f_{\mathrm{L}}^\dagger)_{jk}(f_{\mathrm{R}})_{1j}\frac{3 - 4b_j + b_j^2 + 2\ln[b_j]}{2(b_j - 1)^3}\right|^2, \qquad (3.13)
\end{aligned}$$

where we define $a \equiv (M_X/m_{h^\pm})^2, b_j \equiv (m_{\ell_j}/m_{h^\pm})^2$, under the assumption $M_X, m_{\nu_{\mathrm{L}}} << m_\ell, m_{h^\pm}$.

Thus the decay ratio is correlated to neutrino mass matrix, Δa_μ and LFV through the Yukawa coupling $f_{\mathrm{L(R)}}$.

3.3 Collider physics

Here we discuss the signature of our model at the LHC 13 TeV. Then we focus on the doubly charged Higgs boson $\Delta^{\pm\pm}$, which decays into the same sign lepton pair with right-handed chirality. Particularly the process $pp \to Z_{\mathrm{R}} \to \Delta^{++}\Delta^{--}$ is interesting since it provides clear four lepton signal where invariant masses of same sign leptons and of four leptons respectively give mass of $\Delta^{\pm\pm}$ and $m_{Z_{\mathrm{R}}}$.[7] This is unlikely

[6] This bound is derived from $\sin^2 2\theta = (2 - 20) \times 10^{-11}$.

[7] The doubly charged Higgs pair can be produced via γ and Z exchange in s-channel. In this paper, we do not discuss these productionprocesses

Table 4 Summary of $\ell_i^- \to \ell_j^- \ell_k^+, \ell_\ell^-$ process and the lower bound of experimental data [124]

Process	(i, j, k, ℓ)	Experimental bounds (90% CL)
$\mu^- \to e^- e^+ e^-$	(2, 1, 1, 1)	$\mathrm{Br}(\mu \to e^- e^+ e^-) < 1.0 \times 10^{-12}$
$\tau^- \to e^- e^+ e^-$	(3, 1, 1, 1)	$\mathrm{Br}(\tau \to e^- e^+ e^-) < 2.7 \times 10^{-8}$
$\tau^- \to \mu^- e^+ e^-$	(3, 2, 1, 1)	$\mathrm{Br}(\tau \to \mu^- e^+ e^-) < 1.8 \times 10^{-8}$
$\tau^- \to e^- \mu^+ \mu^-$	(3, 1, 2, 1)	$\mathrm{Br}(\tau \to e^- \mu^+ e^-) < 1.5 \times 10^{-8}$
$\tau^- \to e^- \mu^+ \mu^-$	(3, 1, 2, 2)	$\mathrm{Br}(\tau \to e^- \mu^+ \mu^-) < 2.7 \times 10^{-8}$
$\tau^- \to \mu^- \mu^+ \mu^-$	(3, 2, 2, 2)	$\mathrm{Br}(\tau \to \mu^- \mu^+ \mu^-) < 2.1 \times 10^{-8}$

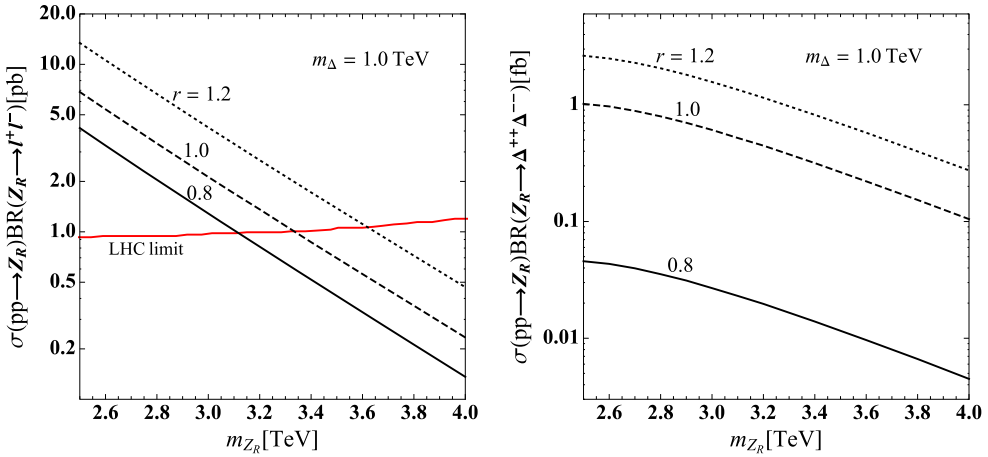

Fig. 1 The *left* and *right plots* show $\sigma(pp \to Z_\mathrm{R})BR(Z_\mathrm{R} \to \ell^+\ell^-)$ and $\sigma(pp \to Z_\mathrm{R})BR(Z_\mathrm{R} \to \Delta^{++}\Delta^{--})$ as a function of Z_R mass for several values of $r \equiv g_\mathrm{R}/g_\mathrm{L}$ where we fixed doubly charged Higgs mass m_Δ as 1 TeV. The *red curve* in the *left plot* indicate the upper limit from LHC experiment [139]

to neither the type II seesaw scenario nor the Zee–Babu type case with $k^{++}e_\mathrm{R}^c e_\mathrm{R}$, because the type II decay mode comes from the left–handed chirality, and the Zee–Babu type doubly charged Higgs is produced via gauge interaction with only $U(1)_Y$. Furthermore each of the component y_{Δ_R} can be determined through the neutrino oscillation data, CLFVs processes, and DM phenomenology such as X-ray line search. Thus we expect that collider signature further test the structure of the Yukawa coupling.

The gauge interactions associated with Z_R are written as [135,136]

$$\mathcal{L} \supset \bar{f}_{SM}\gamma_\mu \left[g_\mathrm{R} c_M \left(Q - \frac{Q_{B-L}}{2c_M^2} \right) Z_\mathrm{R}^\mu \right] f_{SM} - \frac{Q_{B-L}}{2} \frac{s_M^2}{c_M} g_\mathrm{R} Z_\mathrm{R}^\mu (\Delta^{++}\partial_\mu \Delta^{--} - \Delta^{--}\partial_\mu \Delta^{++}) \tag{3.14}$$

where Q is electric charge, Q_{B-L} is $U(1)_{B-L}$ charge, $c_M \equiv \cos\theta_M = \tan\theta_W g_\mathrm{L}/g_\mathrm{R}$, $s_M \equiv \sin\theta_M$, and g_R is $SU(2)_\mathrm{R}$ gauge coupling. Then we estimate the production cross section of Z_R and its branching ratio (BR) with CalcHEP [137] implementing the interaction and applying `CTEQ6L` PDF [138]. In Fig. 1, we show $\sigma(pp \to Z_\mathrm{R})BR(Z_\mathrm{R} \to \ell^+\ell^-)$ and $\sigma(pp \to Z_\mathrm{R})BR(Z_\mathrm{R} \to \Delta^{++}\Delta^{--})$ as a function of m_{Z_R} for several values of $r \equiv g_\mathrm{R}/g_\mathrm{L}$ with fixed doubly charged Higgs mass $m_\Delta = 1$ TeV where constraint on $\sigma(pp \to Z_\mathrm{R})BR(Z_\mathrm{R} \to \ell^+\ell^-)$ from LHC experiment is indicated by red curve [139]. We find that Z_R should be heavier than around 3.5 TeV where the lower mass limit depends on r. Note here that this result does not depend on doubly charged Higgs mass strongly if it is lighter than $m_{Z_\mathrm{R}}/2$ sufficiently. The doubly charged Higgs pair production cross section via Z_R is given as $\sim \{0.28, 0.11, 0.045\}$[fb] for $r = \{1.2, 1.0, 0.8\}$ with $m_{Z_\mathrm{R}} = 4$ TeV. Thus $O(10)$–$O(100)$ number of events can be obtained with luminosity of $\sim$ 100–300 fb^{-1} for $r \geq 1$ while number of events is smaller for $r < 1$. Therefore we can test our model at the LHC with sufficient luminosity since the four lepton final state gives clear signal, and structure of the Yukawa coupling y_{Δ_R} would be investigated by measuring the BR of $\Delta^{\pm\pm}$. The detailed simulation analysis including SM background is beyond the scope of our paper and it will be investigated in future work.

Footnote 7 continued
since they are small as < 0.1 fb for TeV scale doubly charged Higgs and signal is less significant due to absence of peak in invariant mass of four leptons.

3.4 Numerical analysis

Now that all the formulas have been provided, we carry out numerical analysis to search for parameter region satisfying all the constraints. First of all, we fix the following parameters in the scalar sector:

$$m_{h_1} = 125\ \text{GeV}, v_{\text{R}}(\approx v_\Delta) = 10^5\ \text{GeV}, m_{\nu_{R,1}} = 7.1\ \text{keV}. \tag{3.15}$$

Before discussing the numerical analysis, we comment on the neutrinoless double beta decay. Once we apply these above values, we can estimate the neutrinoless double beta decay as

$$m_{\beta\beta} \approx 3.5\ \text{meV}, \tag{3.16}$$

where non-standard contribution is about $\mathcal{O}(10^{-5})$ meV. It suggests that it satisfies the experimental bound on $m_{\beta\beta} \lesssim 0.29$ eV, as discussed before. Then we have 26 free parameters (see Appendix A) and randomly select the values of these parameters within the following ranges:

$$\begin{aligned}
&M_{\text{E},i} = (500\ \text{GeV}, 1000\ \text{GeV})\,,\\
&\quad m_{\nu_{\text{R}},j} = (5000\ \text{GeV}, 10{,}000\ \text{GeV})\,,\\
&\quad m_{h_2} = (1000\ \text{GeV}, 10000\ \text{GeV})\,,\\
&F_{\text{L}_{23}} = (0, 0.01)\,, h_{\text{L}_{11}} = (0, 0.01)\,, h_{\text{L}_{12}} = (0, 0.01)\,,\\
&\quad h_{\text{L}_{13}} = (0, 1)\,,\\
&F_{\text{R}_{23}} = (-0.01, 0)\,, h_{\text{R}_{11}} = (-0.01, 0)\,,\\
&\quad h_{\text{R}_{12}} = (-0.01, 0)\,, h_{\text{R}_{13}} = (-1, 0)\,,\\
&\alpha_1 = (-0.3, -0.2)\,, \alpha_2 = (0.2, 0.3)\,,\\
&\quad \alpha_3 = (-0.0002, -0.00002)\,,\\
&y^i_\Delta = (-0.1, 0.1)\,, \alpha_{\text{R}_1} = (2.9, \pi)\,, \alpha_{R_2} = (1.5, 2)\,,\\
&\quad \alpha_{\text{R}_3} = (0.1, 0.5)\,,\\
&\alpha_{\text{I}} = (-3, -2)\,, \alpha_{\text{p}} = (0.05, 0.1)\,,
\end{aligned} \tag{3.17}$$

which are found as the preferred parameter range to satisfy the constraints.

Then we have examined 10^6 sampling points to investigate how much parameter space is allowed. We find 311 points that satisfy the current LFV constraints and the neutrino oscillation data. Figure 2 shows the correlation between Δa_μ and $\frac{\Gamma(X\to\nu_k\gamma)}{M_X}$ where a red point represents negative Δa_μ and the blue points represent positive Δa_μ. The DM decay rate can satisfy the experimental data (16 points) if the points are within the line between the two black horizontal lines in Fig. 2. On the other hand, the discrepancy of muon $g-2$ from SM is at most the order 10^{-11}, which is too small to explain the experimental data by the order 0.01 magnitude. This is because there exist more negative contributions in Eqs. (III.5–7) than the positive contribution in Eqs. (III.4). But a future experiment might verify the scale.

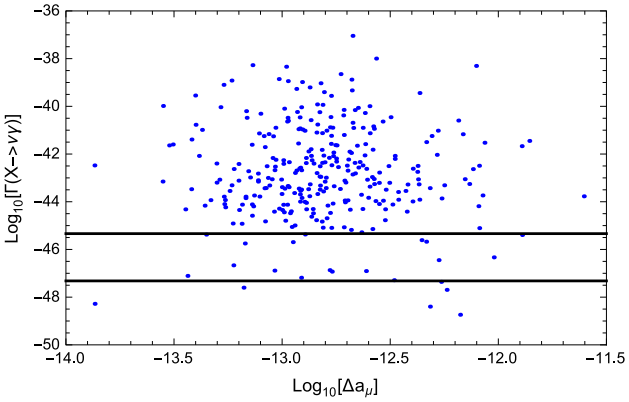

Fig. 2 The correlation between Δa_μ and $\frac{\Gamma(X\to\nu_k\gamma)}{M_X}$. All points satisfy the current LFV constraints, a *red point* means Δa_μ is negative and *blue points* mean Δa_μ is positive. The total number of the consistent data points is 311

4 Conclusions

We have studied a radiative seesaw model based on a $SU(2)_{\text{L}} \times SU(2)_{\text{R}} \times U(1)_{\text{B-L}}$ symmetry, where the neutrino mass matrix is induced at two-loop level. Then we have formulated masses in lepton sector, lepton flavor violating decay ratios, muon $g-2$, and the decay rate of the long-lived dark matter. Due to the antisymmetric Yukawa couplings contributing to the active neutrino mass and absence of Δ_{L}, a zero mass eigenstate (with two massive) is predicted, and (a long-lived) dark matter candidate can be accommodated in our model. Then we have carried out a numerical analysis to search for the parameter space which is consistent with all the experimental constraints, and correlation between Δa_μ and $\Gamma(X \to \nu_k\gamma)/M_X$ for the allowed parameter set is depicted in Fig. 2, in which the red points represent negative Δa_μ and the blue points represent positive Δa_μ. The DM decay rate satisfies the experimental data (16 points) if the points are within the line between the two black horizontal lines. On the other hand, the discrepancy of muon $g-2$ from SM is at most the order 10^{-11} that is too small to explain the current experimental data by the order 0.01 magnitude, since there exists only a positive contribution to be compared with three negative contributions. But a future experiment might verify the scale.

Our model also could be tested at collider experiments by searching for exotic charged particles such as heavy leptons and doubly/singly charged Higgs bosons. These particles would be produced via electroweak interactions at the LHC when their masses are $O(100)$ GeV to $O(1)$ TeV. Then we have analyzed doubly charged Higgs production via the process $pp \to Z_{\text{R}} \to \Delta^{++}\Delta^{--}$ at the LHC where doubly charged Higgs decays into two same sign leptons providing clear signals from four lepton final states. The production cross section is estimated as $\sim$ 0.05–0.3 fb for $m_{Z_{\text{R}}} = 4$

TeV depending on value of the ratio of $SU(2)_{\mathrm{L(R)}}$ gauge couplings, and we can obtain around 10 to 100 number of events with luminosity of $O(100)$ fb^{-1}. Thus we can test the signature of our model and structure of Yukawa coupling for Δ_{R} and right-handed charged leptons could be tested by measuring branching ratio of doubly charged Higgs. The detailed analysis including SM background will be left as future work.

Acknowledgements The authors thank Dr. Kei Yagyu for fruitful discussions. H.O. expresses his sincere gratitude toward all the KIAS members, Korean cordial persons, foods, culture, weather, and all the other things. This work was supported by the Korea Neutrino Research Center which is established by the National Research Foundation of Korea (NRF) Grant funded by the Korea government (MSIP) (No. 2009-0083526) (Y.O.).

Appendix A: Yukawa couplings

In this section, we discuss the structure of Yukawa couplings of our model. Our neutrino masses are obtained by $(\mathcal{M}_\nu)_{ab} \approx m_{\mathrm{D}} m_{\nu_{\mathrm{R}}}^{-1} m_{\mathrm{D}}^{\mathrm{T}}$, where $m_{\nu_{\mathrm{R}}} = y_{\Delta_{\mathrm{R}}} v_\Delta$ and m_{D} is given by Eq. (2.15). Using the Casas–Ibarra parametrization, the m_{D} is written by

$$m_{\mathrm{D}} = U^*_{MNS}.diag\left(m_1^{\frac{1}{2}}, m_2^{\frac{1}{2}}, m_3^{\frac{1}{2}}\right).O.m_{\nu_{\mathrm{R}}}^{\frac{1}{2}}, \tag{A.1}$$

where U_{MNS} is the MNS matrix, m_i's are neutrino masses, O is a complex orthogonal matrix. O is parametrized by three complex parameters: $\alpha_1, \alpha_2, \alpha_3$.

Generally, a matrix M is factorized by the following form:

$$M = LDU, \tag{A.2}$$

where D is diagonal matrix and $L(U)$ is upper (lower) triangular matrix with unit diagonal components. The factorization is called the LDU decomposition. We can factorize m_{D} using the LDU decomposition as follows:

$$m_{\mathrm{D}} = LDU = L_{\mathrm{D}} U_{\mathrm{D}}, \tag{A.3}$$

where $L_{\mathrm{D}} \equiv LD^{\frac{1}{2}} = F_{\mathrm{L}} h_{\mathrm{L}} Z_{\mathrm{D}}^{\frac{1}{2}}$, $U_{\mathrm{D}} \equiv D^{\frac{1}{2}} U = (F_{\mathrm{R}} h_{\mathrm{R}} Z_{\mathrm{D}}^{\frac{1}{2}})^{\mathrm{T}}$ and the diagonal matrix Z_{D} is written by

$$Z_{\mathrm{D}_{ii}} = \frac{v_{\mathrm{L}} v_{\mathrm{R}} \ln Z_i}{2\pi^2 M_{\mathrm{E}_i}(1 - Z_i)}. \tag{A.4}$$

We assume $F_{\mathrm{L}} h_{\mathrm{L}}$ and $F_{\mathrm{R}} h_{\mathrm{R}}$ are lower triangular matrices. The components of $F_{\mathrm{L(R)}}$ and $h_{\mathrm{L(R)}}$ are written in the following form:

$$\begin{aligned}
h_{\mathrm{L(R)}_{31}} &= l_{\mathrm{L(R)}_{21}} - \frac{l_{\mathrm{L(R)}_{22}}}{l_{\mathrm{L(R)}_{32}}} \frac{l_{\mathrm{L(R)}_{11}} l_{\mathrm{L(R)}_{32}}}{l_{\mathrm{L(R)}_{31}} l_{\mathrm{L(R)}_{22}} - l_{\mathrm{L(R)}_{21}} l_{\mathrm{L(R)}_{32}}} h_{\mathrm{L(R)}_{11}}, \\
h_{\mathrm{L(R)}_{21}} &= -l_{\mathrm{L(R)}_{31}} + \frac{l_{\mathrm{L(R)}_{11}} l_{\mathrm{L(R)}_{32}}}{l_{\mathrm{L(R)}_{31}} l_{\mathrm{L(R)}_{22}} - l_{\mathrm{L(R)}_{21}} l_{\mathrm{L(R)}_{32}}} h_{\mathrm{L(R)}_{11}}, \\
h_{\mathrm{L(R)}_{32}} &= l_{\mathrm{L(R)}_{22}} - \frac{l_{\mathrm{L(R)}_{22}}}{l_{\mathrm{L(R)}_{32}}} \frac{l_{\mathrm{L(R)}_{11}} l_{\mathrm{L(R)}_{32}}}{l_{\mathrm{L(R)}_{31}} l_{\mathrm{L(R)}_{22}} - l_{\mathrm{L(R)}_{21}} l_{\mathrm{L(R)}_{32}}} h_{\mathrm{L(R)}_{12}}, \\
h_{\mathrm{L(R)}_{22}} &= -l_{\mathrm{L(R)}_{32}} + \frac{l_{\mathrm{L(R)}_{11}} l_{\mathrm{L(R)}_{32}}}{l_{\mathrm{L(R)}_{31}} l_{\mathrm{L(R)}_{22}} - l_{\mathrm{L(R)}_{21}} l_{\mathrm{L(R)}_{32}}} h_{\mathrm{L(R)}_{12}}, \\
h_{\mathrm{L(R)}_{23}} &= \frac{l_{\mathrm{L(R)}_{11}} l_{\mathrm{L(R)}_{32}}}{l_{\mathrm{L(R)}_{31}} l_{\mathrm{L(R)}_{22}} - l_{\mathrm{L(R)}_{21}} l_{\mathrm{L(R)}_{32}}} h_{\mathrm{L(R)}_{13}}, \\
h_{\mathrm{L(R)}_{33}} &= \frac{h_{\mathrm{L(R)}_{23}} h_{\mathrm{L(R)}_{32}}}{h_{\mathrm{L(R)}_{22}}}, \\
F_{\mathrm{L(R)}_{12}} &= F_{\mathrm{L(R)}_{23}} \frac{h_{\mathrm{L(R)}_{23}} h_{\mathrm{L(R)}_{32}}}{h_{\mathrm{L(R)}_{13}} h_{\mathrm{L(R)}_{22}}} \\
F_{\mathrm{L(R)}_{13}} &= -F_{\mathrm{L(R)}_{23}} \frac{h_{\mathrm{L(R)}_{23}}}{h_{\mathrm{L(R)}_{13}}}.
\end{aligned} \tag{A.5}$$

In this case, $F_{\mathrm{L(R)}} h_{\mathrm{L(R)}}$ becomes a lower triangular matrix:

$$F_{\mathrm{L(R)}} h_{\mathrm{L(R)}} = \begin{pmatrix} l_{\mathrm{L(R)}_{11}} & 0 & 0 \\ l_{\mathrm{L(R)}_{21}} & l_{\mathrm{L(R)}_{22}} & 0 \\ l_{\mathrm{L(R)}_{31}} & l_{\mathrm{L(R)}_{32}} & l_{L(R)_{33}} \end{pmatrix} = L_{\mathrm{D}} \text{ or } U_{\mathrm{D}}^{\mathrm{T}}. \tag{A.6}$$

$l_{\mathrm{L(R)}_{ij}}$ are determined by neutrino oscillation experiments. Therefore we have eight free parameters: $h_{\mathrm{L(R)}_{11}}$, $h_{\mathrm{L(R)}_{12}}$, $h_{\mathrm{L(R)}_{13}}$ and $F_{\mathrm{L(R)}_{23}}$.

Appendix B Loop factors for $\ell_i^- \to \ell_j^- \ell_k^+ \ell_\ell^-$

Here we summarize the loop factors appearing in the formula of lepton flavor violating decay $\ell_i^- \to \ell_j^- \ell_k^+ \ell_\ell^-$ in Eq. (3.12).

$$A = \frac{-i}{2(4\pi)^2}\int \mathrm{d}X \sum_{\alpha=1}^{3}\sum_{a=1}^{2} \frac{(H^b)_{\ell\alpha}(H_a^\dagger)_{\alpha i}(H^a)_{j\beta}(H_b^\dagger)_{\beta k} - (H^b)_{\ell\alpha}(H_a^\dagger)_{\alpha i}(H^b)_{j\beta}(H_a^\dagger)_{\beta k}}{x_1 M_{E_\alpha}^2 + x_2 M_{E_\beta}^2 + x_3 m_{h_a}^2 + x_4 m_{h_b}^2}, \tag{B.1}$$

$$B = \frac{-i}{2(4\pi)^2}\int \mathrm{d}X \sum_{\alpha=1}^{3}\sum_{a=1}^{2} \frac{(H^a)_{\ell\beta}(H_b^\dagger)_{\beta k}(H^b)_{j\alpha}(H_a^\dagger)_{\alpha i} - (H^b)_{\ell\beta}(H_a^\dagger)_{\beta k}(H^b)_{j\alpha}(H_a^\dagger)_{\alpha i}}{x_1 M_{E_\alpha}^2 + x_2 M_{E_\beta}^2 + x_3 m_{h_a}^2 + x_4 m_{h_b}^2}, \tag{B.2}$$

$$C = \frac{i}{(4\pi)^2}\int \mathrm{d}X \sum_{\alpha=1}^{3}\sum_{a=1}^{2} \frac{M_{E_\alpha}M_{E_\beta}((H^b)_{\ell\alpha}(H_a^\dagger)_{\alpha i}(H^a)_{j\beta}(H_b^\dagger)_{\beta k} + (H^b)_{\ell\alpha}(H_a^\dagger)_{\alpha i}(H^b)_{j\beta}(H_a^\dagger)_{\beta k})}{(x_1 M_{E_\alpha}^2 + x_2 M_{E_\beta}^2 + x_3 m_{h_a}^2 + x_4 m_{h_b}^2)^2}, \tag{B.3}$$

$$D = \frac{i}{(4\pi)^2}\int \mathrm{d}X \sum_{\alpha=1}^{3}\sum_{a=1}^{2} \frac{M_{E_\alpha}M_{E_\beta}((H^a)_{\ell\beta}(H_b^\dagger)_{\beta k}(H^b)_{j\alpha}(H_a^\dagger)_{\alpha i} + (H^b)_{\ell\beta}(H_a^\dagger)_{\beta k}(H^b)_{j\alpha}(H_a^\dagger)_{\alpha i})}{(x_1 M_{E_\alpha}^2 + x_2 M_{E_\beta}^2 + x_3 m_{h_a}^2 + x_4 m_{h_b}^2)^2}, \tag{B.4}$$

$$A_{\mathrm{L}} = \frac{4i(f_{\mathrm{L}}f_{\mathrm{L}}^\dagger)_{ij}(f_{\mathrm{L}}f_{\mathrm{L}}^\dagger)_{k\ell}}{(4\pi)^2 m_{h^\pm}^2} - \frac{i}{2(4\pi)^2}\int \mathrm{d}X \sum_{\alpha=1}^{3}\sum_{a=1}^{2} \frac{M_{E_\alpha}M_{E_\beta}\,(d + h(\ell \leftrightarrow j))}{(x_1 M_{E_\alpha}^2 + x_2 M_{E_\beta}^2 + x_3 m_{h_a}^2 + x_4 m_{A_b}^2)^2}, \tag{B.5}$$

$$B_{\mathrm{L}} = -\frac{4i(f_{\mathrm{L}}f_{\mathrm{L}}^\dagger)_{i\ell}(f_{\mathrm{L}}f_{\mathrm{L}}^\dagger)_{kj}}{(4\pi)^2 m_{h^\pm}^2}, \tag{B.6}$$

$$\begin{aligned} A_{\mathrm{R}} = {} & \frac{-i}{2(4\pi)^2}\int \mathrm{d}X \sum_{\alpha=1}^{3}\sum_{a=1}^{2} \frac{(H'^a)_{\ell\beta}(H_b'^\dagger)_{\beta k}(H'^b)_{j\alpha}(H_a'^\dagger)_{\alpha i} - (H'^b)_{\ell\beta}(H_a'^\dagger)_{\beta k}(H'^b)_{j\alpha}(H_a'^\dagger)_{\alpha i}}{x_1 M_{E_\alpha}^2 + x_2 M_{E_\beta}^2 + x_3 m_{A_a}^2 + x_4 m_{A_b}^2} \\ & + \frac{i}{2(4\pi)^2}\int \mathrm{d}X \sum_{\alpha=1}^{3}\sum_{a=1}^{2} \frac{e + f - g - h}{x_1 M_{E_\alpha}^2 + x_2 M_{E_\beta}^2 + x_3 m_{h_a}^2 + x_4 m_{A_b}^2} \\ & - \frac{i}{2(4\pi)^2}\int \mathrm{d}X \sum_{\alpha=1}^{3}\sum_{a=1}^{2} \frac{M_{E_\alpha}M_{E_\beta}\,(c + g(\ell \leftrightarrow j))}{(x_1 M_{E_\alpha}^2 + x_2 M_{E_\beta}^2 + x_3 m_{h_a}^2 + x_4 m_{A_b}^2)^2} + 8i(f_{\mathrm{R}})_{a\ell}(f_{\mathrm{R}})_{a'j}(f_{\mathrm{R}}^\dagger)_{ka}(f_{\mathrm{R}}^\dagger)_{ia'}J_{1,aa'}, \end{aligned} \tag{B.7}$$

$$\begin{aligned} B_{\mathrm{R}} = {} & \frac{-i}{2(4\pi)^2}\int \mathrm{d}X \sum_{\alpha=1}^{3}\sum_{a=1}^{2} \frac{(H'^b)_{\ell\alpha}(H_a'^\dagger)_{\alpha i}(H'^a)_{j\beta}(H_b'^\dagger)_{\beta k} - (H'^b)_{\ell\alpha}(H_a'^\dagger)_{\alpha i}(H'^b)_{j\beta}(H_a'^\dagger)_{\beta k}}{x_1 M_{E_\alpha}^2 + x_2 M_{E_\beta}^2 + x_3 m_{A_a}^2 + x_4 m_{A_b}^2} \\ & + \frac{i}{2(4\pi)^2}\int \mathrm{d}X \sum_{\alpha=1}^{3}\sum_{a=1}^{2} \frac{a + b - c - d}{x_1 M_{E_\alpha}^2 + x_2 M_{E_\beta}^2 + x_3 m_{h_a}^2 + x_4 m_{A_b}^2} - 8i(f_{\mathrm{R}})_{a\ell}(f_{\mathrm{R}})_{a'j}(f_{\mathrm{R}}^\dagger)_{ka'}(f_{\mathrm{R}}^\dagger)_{ia}J_{1,aa'}, \end{aligned} \tag{B.8}$$

$$C_{\mathrm{R}} = 16i m_{\nu_{R,a}} m_{\nu_{R,a'}}(f_{\mathrm{R}})_{a\ell}(f_{\mathrm{R}})_{aj}(f_{\mathrm{R}}^\dagger)_{ka'}(f_{\mathrm{R}}^\dagger)_{ia'}J_{2,aa'}, \tag{B.9}$$

$$E = \frac{i}{2(4\pi)^2}\int \mathrm{d}X \sum_{\alpha=1}^{3}\sum_{a=1}^{2} \times \frac{M_{E_\alpha}M_{E_\beta}\,(a + e(\ell \leftrightarrow j))}{(x_1 M_{E_\alpha}^2 + x_2 M_{E_\beta}^2 + x_3 m_{h_a}^2 + x_4 m_{A_b}^2)^2}, \tag{B.10}$$

$$F = \frac{i}{2(4\pi)^2}\int \mathrm{d}X \sum_{\alpha=1}^{3}\sum_{a=1}^{2} \times \frac{M_{E_\alpha}M_{E_\beta}\,(b + f(\ell \leftrightarrow j))}{(x_1 M_{E_\alpha}^2 + x_2 M_{E_\beta}^2 + x_3 m_{h_a}^2 + x_4 m_{A_b}^2)^2}. \tag{B.11}$$

Here the factors $\{a, b, \ldots, h\}$ have been defined as

$$\begin{aligned} a &= (H'^b)_{\ell\alpha}(H_a^\dagger)_{\alpha i}(H^a)_{j\beta}(H_b'^\dagger)_{\beta k}, \\ b &= (H^a)_{\ell\alpha}(H_b'^\dagger)_{\alpha i}(H'^b)_{j\beta}(H_a^\dagger)_{\beta k}, \\ c &= (H'^b)_{\ell\alpha}(H_a^\dagger)_{\alpha i}(H'^b)_{j\beta}(H_a^\dagger)_{\beta k}, \\ d &= (H^a)_{\ell\alpha}(H_b'^\dagger)_{\alpha i}(H^a)_{j\beta}(H_b'^\dagger)_{\beta k}, \\ e &= (H^a)_{\ell\beta}(H_b'^\dagger)_{\beta k}(H'^b)_{j\alpha}(H_a^\dagger)_{\alpha i}, \\ f &= (H'^b)_{\ell\beta}(H_a^\dagger)_{\beta k}(H^a)_{j\alpha}(H_b'^\dagger)_{\alpha i}, \end{aligned} \tag{B.12–B.14}$$

$$g = (H'^{b})_{\ell\beta}(H_a^{\dagger})_{\beta k}(H'^{b})_{j\alpha}(H_a^{\dagger})_{\alpha i},$$
$$h = (H^{a})_{\ell\beta}(H_b'^{\dagger})_{\beta k}(H^{a})_{j\alpha}(H_b'^{\dagger})_{\alpha i}, \tag{B.15}$$
$$J_{i,aa'} \equiv \frac{1}{(4\pi)^2}\int_0^1 \mathrm{d}x \int_0^{1-x} \mathrm{d}y \times \frac{1-x-y}{[x m^2_{\nu_{\mathrm{R}},a} + y m^2_{\nu_{\mathrm{R}},a'} + (1-x-y)m^2_{h^\pm}]^i}, \quad i = (1,2), \tag{B.16}$$

where we define the coupling factors $H^a_{ij} \equiv \frac{(h_{\mathrm{L}})_{ij}(O_{\mathrm{R}}^{\mathrm{T}})_{1a} + (h_{\mathrm{R}})_{ij}(O_{\mathrm{R}}^{\mathrm{T}})_{2a}}{2\sqrt{2}}$ and $H'^a_{ij} \equiv \frac{(O_I^{\mathrm{T}})_{1a}(h_{\mathrm{R}})_{ij}}{\sqrt{2}}$, $\int \mathrm{d}X \equiv \int_0^1 \mathrm{d}x_1\mathrm{d}x_2\mathrm{d}x_3\mathrm{d}x_4\delta(x_1+x_2+x_3+x_4-1)$.

References

1. D.V. Forero, M. Tortola, J.W.F. Valle, Phys. Rev. D **90**(9), 093006 (2014). arXiv:1405.7540 [hep-ph]
2. R.N. Mohapatra, J.C. Pati, Phys. Rev. D **11**, 566 (1975)
3. A. Zee, Phys. Lett. B **93**, 389 (1980). **(Erratum-ibid. B 95, 461 (1980))**
4. T.P. Cheng, L.F. Li, Phys. Rev. D **22**, 2860 (1980)
5. A. Zee, Nucl. Phys. B **264**, 99 (1986)
6. K.S. Babu, Phys. Lett. B **203**, 132 (1988)
7. L.M. Krauss, S. Nasri, M. Trodden, Phys. Rev. D **67**, 085002 (2003). arXiv:hep-ph/0210389
8. E. Ma, Phys. Rev. D **73**, 077301 (2006). arXiv:hep-ph/0601225
9. M. Aoki, S. Kanemura, O. Seto, Phys. Rev. Lett. **102**, 051805 (2009). arXiv:0807.0361
10. M. Gustafsson, J.M. No, M.A. Rivera, Phys. Rev. Lett. **110**, 211802 (2013). arXiv:1212.4806 [hep-ph]
11. T. Hambye, K. Kannike, E. Ma, M. Raidal, Phys. Rev. D **75**, 095003 (2007). arXiv:hep-ph/0609228
12. P.-H. Gu, U. Sarkar, Phys. Rev. D **77**, 105031 (2008). arXiv:0712.2933 [hep-ph]
13. N. Sahu, U. Sarkar, Phys. Rev. D **78**, 115013 (2008). arXiv:0804.2072 [hep-ph]
14. P.-H. Gu, U. Sarkar, Phys. Rev. D **78**, 073012 (2008). arXiv:0807.0270 [hep-ph]
15. P. Fileviez Perez, C. Murgui, S. Ohmer, Phys. Rev. D **94**(5), 051701 (2016). doi:10.1103/PhysRevD.94.051701. arXiv:1607.00246 [hep-ph]
16. K.S. Babu, C. Macesanu, Phys. Rev. D **67**, 073010 (2003). arXiv:hep-ph/0212058
17. D. Aristizabal Sierra, D. Restrepo, JHEP **0608**, 036 (2006). arXiv:hep-ph/0604012
18. D. Aristizabal Sierra, M. Hirsch, JHEP **0612**, 052 (2006). arXiv:hep-ph/0609307
19. M. Nebot, J.F. Oliver, D. Palao, A. Santamaria, Phys. Rev. D **77**, 093013 (2008). arXiv:0711.0483 [hep-ph]
20. R. Bouchand, A. Merle, JHEP **1207**, 084 (2012). arXiv:1205.0008 [hep-ph]
21. Y. Kajiyama, H. Okada, K. Yagyu, Nucl. Phys. B **887**, 358 (2014). arXiv:1309.6234 [hep-ph]
22. K.L. McDonald, JHEP **1311**, 131 (2013). arXiv:1310.0609 [hep-ph]
23. E. Ma, Phys. Lett. B **732**, 167 (2014). arXiv:1401.3284 [hep-ph]
24. D. Schmidt, T. Schwetz, H. Zhang, Nucl. Phys. B **885**, 524 (2014). arXiv:1402.2251 [hep-ph]
25. J. Herrero-Garcia, M. Nebot, N. Rius, A. Santamaria, Nucl. Phys. B **885**, 542 (2014). arXiv:1402.4491 [hep-ph]
26. A. Ahriche, S. Nasri, R. Soualah, Phys. Rev. D **89**, 095010 (2014). arXiv:1403.5694 [hep-ph]
27. H.N. Long, V.V. Vien, Int. J. Mod. Phys. A **29**(13), 1450072 (2014). arXiv:1405.1622 [hep-ph]
28. V. Van Vien, H.N. Long, P.N. Thu, arXiv:1407.8286 [hep-ph]
29. M. Aoki, S. Kanemura, T. Shindou, K. Yagyu, JHEP **1007**, 084 (2010). arXiv:1005.5159 [hep-ph]. **(Erratum-ibid. 1011, 049 (2010))**
30. S. Kanemura, O. Seto, T. Shimomura, Phys. Rev. D **84**, 016004 (2011). arXiv:1101.5713 [hep-ph]
31. M. Lindner, D. Schmidt, T. Schwetz, Phys. Lett. B **705**, 324 (2011). arXiv:1105.4626 [hep-ph]
32. S. Kanemura, T. Nabeshima, H. Sugiyama, Phys. Lett. B **703**, 66 (2011). arXiv:1106.2480 [hep-ph]
33. M. Aoki, J. Kubo, T. Okawa, H. Takano, Phys. Lett. B **707**, 107 (2012). arXiv:1110.5403 [hep-ph]
34. S. Kanemura, T. Nabeshima, H. Sugiyama, Phys. Rev. D **85**, 033004 (2012). arXiv:1111.0599 [hep-ph]
35. D. Schmidt, T. Schwetz, T. Toma, Phys. Rev. D **85**, 073009 (2012). arXiv:1201.0906 [hep-ph]
36. S. Kanemura, H. Sugiyama, Phys. Rev. D **86**, 073006 (2012). arXiv:1202.5231 [hep-ph]
37. Y. Farzan, E. Ma, Phys. Rev. D **86**, 033007 (2012). arXiv:1204.4890 [hep-ph]
38. K. Kumericki, I. Picek, B. Radovcic, JHEP **1207**, 039 (2012). arXiv:1204.6597 [hep-ph]
39. K. Kumericki, I. Picek, B. Radovcic, Phys. Rev. D **86**, 013006 (2012). arXiv:1204.6599 [hep-ph]
40. E. Ma, Phys. Lett. B **717**, 235 (2012). arXiv:1206.1812 [hep-ph]
41. G. Gil, P. Chankowski, M. Krawczyk, Phys. Lett. B **717**, 396 (2012). arXiv:1207.0084 [hep-ph]
42. H. Okada, T. Toma, Phys. Rev. D **86**, 033011 (2012). arXiv:1207.0864 [hep-ph]
43. D. Hehn, A. Ibarra, Phys. Lett. B **718**, 988 (2013). arXiv:1208.3162 [hep-ph]
44. S. Baek, P. Ko, H. Okada, E. Senaha, JHEP **1409**, 153 (2014). arXiv:1209.1685 [hep-ph]
45. P.S.B. Dev, A. Pilaftsis, Phys. Rev. D **86**, 113001 (2012). arXiv:1209.4051 [hep-ph]
46. Y. Kajiyama, H. Okada, T. Toma, Eur. Phys. J. C **73**, 2381 (2013). arXiv:1210.2305 [hep-ph]
47. M. Kohda, H. Sugiyama, K. Tsumura, Phys. Lett. B **718**, 1436 (2013). arXiv:1210.5622 [hep-ph]
48. M. Aoki, J. Kubo, H. Takano, Phys. Rev. D **87**(11), 116001 (2013). arXiv:1302.3936 [hep-ph]
49. Y. Kajiyama, H. Okada, K. Yagyu, Nucl. Phys. B **874**, 198 (2013). arXiv:1303.3463 [hep-ph]
50. Y. Kajiyama, H. Okada, T. Toma, Phys. Rev. D **88**, 015029 (2013). arXiv:1303.7356]
51. S. Kanemura, T. Matsui, H. Sugiyama, Phys. Lett. B **727**, 151 (2013). arXiv:1305.4521 [hep-ph]
52. S.S.C. Law, K.L. McDonald, JHEP **1309**, 092 (2013). arXiv:1305.6467 [hep-ph]
53. B. Dasgupta, E. Ma, K. Tsumura, Phys. Rev. D **89**, 041702 (2014). arXiv:1308.4138 [hep-ph]
54. S. Baek, H. Okada, T. Toma, JCAP **1406**, 027 (2014). arXiv:1312.3761 [hep-ph]
55. S. Baek, H. Okada, arXiv:1403.1710 [hep-ph]
56. H. Okada, arXiv:1404.0280 [hep-ph]
57. A. Ahriche, C.S. Chen, K.L. McDonald, S. Nasri, Phys. Rev. D **90**(1), 015024 (2014). arXiv:1404.2696 [hep-ph]
58. A. Ahriche, K.L. McDonald, S. Nasri, JHEP **1410**, 167 (2014). arXiv:1404.5917 [hep-ph]

59. C.-S. Chen, K.L. McDonald, S. Nasri, Phys. Lett. B **734**, 388 (2014). arXiv:1404.6033 [hep-ph]
60. S. Kanemura, T. Matsui, H. Sugiyama, Phys. Rev. D **90**, 013001 (2014). arXiv:1405.1935 [hep-ph]
61. H. Okada, Y. Orikasa, Phys. Rev. D **90**(7), 075023 (2014). arXiv:1407.2543 [hep-ph]
62. S. Fraser, E. Ma, O. Popov, Phys. Lett. B **737**, 280 (2014). arXiv:1408.4785 [hep-ph]
63. H. Okada, T. Toma, K. Yagyu, Phys. Rev. D **90**(9), 095005 (2014). arXiv:1408.0961 [hep-ph]
64. H. Hatanaka, K. Nishiwaki, H. Okada, Y. Orikasa, Nucl. Phys. B **894**, 268 (2015). arXiv:1412.8664 [hep-ph]
65. S. Baek, H. Okada, K. Yagyu, JHEP **1504**, 049 (2015). arXiv:1501.01530 [hep-ph]
66. L.G. Jin, R. Tang, F. Zhang, Phys. Lett. B **741**, 163 (2015). arXiv:1501.02020 [hep-ph]
67. P. Culjak, K. Kumericki, I. Picek, Phys. Lett. B **744**, 237 (2015). arXiv:1502.07887 [hep-ph]
68. H. Okada, arXiv:1503.04557 [hep-ph]
69. C.Q. Geng, L.H. Tsai, arXiv:1503.06987 [hep-ph]
70. H. Okada, N. Okada, Y. Orikasa, arXiv:1504.01204 [hep-ph]
71. C.Q. Geng, D. Huang, L.H. Tsai, Phys. Lett. B **745**, 56 (2015). arXiv:1504.05468 [hep-ph]
72. A. Ahriche, K.L. McDonald, S. Nasri, T. Toma, Phys. Lett. B **746**, 430 (2015). arXiv:1504.05755 [hep-ph]
73. D. Restrepo, A. Rivera, M. Sánchez-Peláez, O. Zapata, W. Tangarife, arXiv:1504.07892 [hep-ph]
74. S. Kashiwase, H. Okada, Y. Orikasa, T. Toma, arXiv:1505.04665 [hep-ph]
75. K. Nishiwaki, H. Okada, Y. Orikasa, arXiv:1507.02412 [hep-ph]
76. W. Wang, Z.L. Han, Phys. Rev. D **92**, 095001 (2015). arXiv:1508.00706 [hep-ph]
77. H. Okada, K. Yagyu, arXiv:1508.01046 [hep-ph]
78. A. Ahriche, K.L. McDonald, S. Nasri, arXiv:1508.02607 [hep-ph]
79. Y.H. Ahn, H. Okada, Phys. Rev. D **85**, 073010 (2012). arXiv:1201.4436 [hep-ph]
80. E. Ma, A. Natale, A. Rashed, Int. J. Mod. Phys. A **27**, 1250134 (2012). arXiv:1206.1570 [hep-ph]
81. Y. Kajiyama, H. Okada, K. Yagyu, JHEP **10**, 196 (2013). arXiv:1307.0480 [hep-ph]
82. A.E. Carcamo Hernandez, I.D.M. Varzielas, S.G. Kovalenko, H. Päs, I. Schmidt. Phys. Rev. D **88**, 076014 (2013). arXiv:1307.6499 [hep-ph]
83. E. Ma, A. Natale, Phys. Lett. B **723**, 403 (2014). arXiv:1403.6772 [hep-ph]
84. M. Aoki, T. Toma, JCAP **1409**, 016 (2014). arXiv:1405.5870 [hep-ph]
85. E. Ma, Phys. Lett. B **741**, 202 (2015). arXiv:1411.6679 [hep-ph]
86. E. Ma, arXiv:1504.02086 [hep-ph]
87. E. Ma, Phys. Rev. Lett. **112**, 091801 (2014). arXiv:1311.3213 [hep-ph]
88. H. Okada, K. Yagyu, Phys. Rev. D **89**, 053008 (2014). arXiv:1311.4360 [hep-ph]
89. S. Baek, H. Okada, T. Toma, Phys. Lett. B **732**, 85 (2014). arXiv:1401.6921 [hep-ph]
90. H. Okada, K. Yagyu, Phys. Rev. D **90**(3), 035019 (2014). arXiv:1405.2368 [hep-ph]
91. V. Brdar, I. Picek, B. Radovcic, Phys. Lett. B **728**, 198 (2014). arXiv:1310.3183 [hep-ph]
92. H. Okada, Y. Orikasa, arXiv:1509.04068 [hep-ph]
93. H. Okada, Y. Orikasa, T. Toma, arXiv:1511.01018 [hep-ph]
94. S. Fraser, C. Kownacki, E. Ma, O. Popov, arXiv:1511.06375 [hep-ph]
95. S. Fraser, E. Ma, M. Zakeri, arXiv:1511.07458 [hep-ph]
96. R. Adhikari, D. Borah, E. Ma, arXiv:1512.05491 [hep-ph]
97. S. Kanemura, H. Sugiyama, Phys. Lett. B **753**, 161 (2016). doi:10.1016/j.physletb.2015.12.012. arXiv:1510.08726 [hep-ph]
98. F. Bonnet, M. Hirsch, T. Ota, W. Winter, JHEP **1207**, 153 (2012). arXiv:1204.5862 [hep-ph]
99. D. Aristizabal Sierra, A. Degee, L. Dorame, M. Hirsch, JHEP **1503**, 040 (2015). arXiv:1411.7038 [hep-ph]
100. H. Davoudiasl, I.M. Lewis, Phys. Rev. D **90**(3), 033003 (2014). arXiv:1404.6260 [hep-ph]
101. M. Lindner, S. Schmidt, J. Smirnov, arXiv:1405.6204 [hep-ph]
102. H. Okada, Y. Orikasa, arXiv:1412.3616 [hep-ph]
103. J. March-Russell, C. McCabe, M. McCullough, JHEP **1003**, 108 (2010). arXiv:0911.4489 [hep-ph]
104. S. F. King, A. Merle, L. Panizzi, arXiv:1406.4137 [hep-ph]
105. Y. Mambrini, S. Profumo, F.S. Queiroz, arXiv:1508.06635 [hep-ph]
106. S.M. Boucenna, S. Morisi, J.W.F. Valle, Adv. High Energy Phys. **2014**, 831598 (2014). doi:10.1155/2014/831598. arXiv:1404.3751 [hep-ph]
107. A. Ahriche, S.M. Boucenna, S. Nasri, arXiv:1601.04336 [hep-ph]
108. H. Okada, Y. Orikasa, arXiv:1512.06687 [hep-ph]
109. A. Ahriche, K.L. McDonald, S. Nasri, I. Picek, arXiv:1603.01247 [hep-ph]
110. S. Kanemura, K. Nishiwaki, H. Okada, Y. Orikasa, S.C. Park, R. Watanabe, arXiv:1512.09048 [hep-ph]
111. T. Nomura, H. Okada, arXiv:1601.00386 [hep-ph]
112. J.H. Yu, arXiv:1601.02609 [hep-ph]
113. R. Ding, Z.L. Han, Y. Liao, X.D. Ma, arXiv:1601.02714 [hep-ph]
114. T. Nomura, H. Okada, arXiv:1601.04516 [hep-ph]
115. H. Okada, K. Yagyu, arXiv:1601.05038 [hep-ph]
116. T. Nomura, H. Okada, arXiv:1601.07339 [hep-ph]
117. P. Ko, T. Nomura, H. Okada, Y. Orikasa, arXiv:1602.07214 [hep-ph]
118. A.E.C. Hernandez, arXiv:1512.09092 [hep-ph]
119. C. Arbelaez, A.E.C. Hernandez, S. Kovalenko, I. Schmidt, arXiv:1602.03607 [hep-ph]
120. W. Chao, arXiv:1512.08484 [hep-ph]
121. R.N. Mohapatra, Phys. Lett. B **201**, 517 (1988)
122. A. Boyarsky, O. Ruchayskiy, D. Iakubovskyi, J. Franse, Phys. Rev. Lett. **113**, 251301 (2014). arXiv:1402.4119 [astro-ph.CO]
123. E. Bulbul, M. Markevitch, A. Foster, R.K. Smith, M. Loewenstein, S.W. Randall, Astrophys. J. **789**, 13 (2014). arXiv:1402.2301 [astro-ph.CO]
124. K.A. Olive et al., Particle Data Group, Chin. Phys. C **38**, 090001 (2014)
125. H.V. Klapdor-Kleingrothaus, I.V. Krivosheina, Mod. Phys. Lett. A **21**, 1547 (2006). doi:10.1142/S0217732306020937
126. G.W. Bennett et al., [Muon G-2 Collaboration], Phys. Rev. D **73**, 072003 (2006). arXiv:hep-ex/0602035
127. F. Jegerlehner, A. Nyffeler, Phys. Rept. **477**, 1 (2009). arXiv:0902.3360 [hep-ph]
128. M. Benayoun, P. David, L. Delbuono, F. Jegerlehner, Eur. Phys. J. C **72**, 1848 (2012). arXiv:1106.1315 [hep-ph]
129. F.S. Queiroz, W. Shepherd, Phys. Rev. D **89**(9), 095024 (2014). arXiv:1403.2309 [hep-ph]
130. J. Adam et al. [MEG Collaboration], Phys. Rev. Lett. **110**, 201801 (2013). arXiv:1303.0754 [hep-ex]
131. A. Pich, Prog. Part. Nucl. Phys. **75**, 41 (2014). arXiv:1310.7922 [hep-ph]
132. F. Bezrukov, H. Hettmansperger, M. Lindner, Phys. Rev. D **81**, 085032 (2010). arXiv:0912.4415 [hep-ph]
133. M. Nemevsek, G. Senjanovic, Y. Zhang, JCAP **1207**, 006 (2012). arXiv:1205.0844 [hep-ph]
134. G. Faisel, S.Y. Ho, J. Tandean, Phys. Lett. B **738**, 380 (2014). arXiv:1408.5887 [hep-ph]

135. P. Duka, J. Gluza, M. Zralek, Ann. Phys. **280**, 336 (2000). arXiv:hep-ph/9910279
136. P. Ko, T. Nomura, Phys. Lett. B **753**, 612 (2016). arXiv:1510.07872 [hep-ph]
137. A. Belyaev, N.D. Christensen, A. Pukhov, Comput. Phys. Commun. **184**, 1729 (2013). arXiv:1207.6082 [hep-ph]
138. P.M. Nadolsky, H.L. Lai, Q.H. Cao, J. Huston, J. Pumplin, D. Stump, W.K. Tung, C.-P. Yuan, Phys. Rev. D **78**, 013004 (2008). arXiv:0802.0007 [hep-ph]
139. M. Aaboud et al. [ATLAS Collaboration], Phys. Lett. B **761**, 372 (2016). arXiv:1607.03669 [hep-ex]